
Article:
Mechleri, E., Brown, S.F. orcid.org/0000-0001-8229-8004, Fennell, P.S. et al. (1 more author) (2017) CO2 capture and storage (CCS) cost reduction via infrastructure right-sizing. Chemical Engineering Research and Design. ISSN 0263-8762

https://doi.org/10.1016/j.cherd.2017.01.016

CO_2 capture and storage (CCS) cost reduction via infrastructure right-sizing

Evgenia Mechleri[a,b], Solomon Brown[c], Paul S. Fennell[d], Niall Mac Dowell[a,b,*]

[a] *Centre for Process Systems Engineering, Imperial College London, South Kensington, London SW7 2AZ UK*
[b] *Centre for Environmental Policy, Imperial College London, South Kensington, London SW7 1NA UK*
[c] *Department of Chemical and Biological Engineering, The University of Sheffield, Mappin Street S1 3JD*
[d] *Department of Chemical Engineering, Imperial College London, South Kensington, UK*

Abstract

Carbon capture and storage (CCS) will be a critical component of a portfolio of low-carbon energy technologies required to combat climate change [1]. As such, an extensive transportation infrastructure will be required to transport captured CO_2 from different sources to the available sinks. Several studies in the literature suggest that shared oversized pipeline networks may be the most efficient long term option compared to single source to sink pipelines, based on increased CCS deployment over the years and therefore increased CO_2 flowrate to the transport network. However, what is neglected in this vision is that the deployment of intermittent renewable energy tends to displace thermal power generation. This directly reduces the amount of fossil fuel burned, CO_2 produced, captured and transported through the network. This paper presents an optimisation methodology to "right-size" CO_2 transport infrastructure, explicitly accounting for the transient flow of CO_2 arising from the co-deployment of intermittent renewable energy generators. By application of this methodology, we demonstrate that capital cost reductions of up to 28% are possible relative to a business-as-usual design case.

Keywords: CO_2 pipeline transport, optimisation, CCS, cost minimisation

*Corresponding author
Email address: niall@imperial.ac.uk (Niall Mac Dowell)

1. Introduction

Carbon capture and storage is considered one of the most promising technological options for the mitigation of CO_2 emissions from the power generation sector and other carbon-intensive sources, and can enable the transition from the current fossil fuel-based economy to a sustainable technology era [2]. However, to date, research efforts have been primarily focused on either the capture or storage elements of the CCS chain. This is understandable to a point, since the transport of CO_2 will have similarities to the natural gas transport pipelines, and therefore can be considered a mature technology. Nevertheless, when considering CO_2 transport there are some technical challenges to be addressed, such as the presence of corrosive elements, in the CO_2 stream, such as H_2O or O_2 which lead to an increased risk of ductile fracture [3], [4], the variability of flow and the need for establishing a single set of standards and specifications for a network where the CO_2 is originated from different sources and capture technologies. Another important challenge is the cost-optimal design of the CO_2 transport system [5]. Benefits associated with economies of scale are a typical feature of large infrastructure projects, such as gas pipelines, electricity transmission lines and telephone lines. It is therefore preferable to build one shared infrastructure rather than several smaller facilities[6]. The prevailing opinion in the academic literature is that CO_2 transport networks will also benefit from significant economies of scale [7]. This is, in part, predicated on the assumption that as CCS plants are large, capital-intensive assets, it would be desirous to operate them in baseload fashion. [6], [8], [9], [10].

In their work, Wang et al. [11], suggested that based on the anticipation that the CO_2 flowrate will increase over time, oversized pipelines are a more economic option than the subsequent deployment of additional CO_2 pipeline capacity in parallel with existing capacity. This is in agreeement with the analysis of Morbee et al. [12], Alhajaj et al. [8] and Middleton and Bielicki[13], who developed an optimisation model capable of predicting the optimal pipeline-

based CO_2 network for pre-specified sources and sinks. They concluded that the oversized design would take advantage of the economies of scale and enable the connection of other CO_2 sources in the future. However, this may not be always the case. When oversizing the CO_2 transport pipeline, it is anticipated that the new decarbonised power plants will be located close to the transport line so as to avoid any excess cost of new connection lines and not close to the electric load or fuel supply. In contrast to these contributions, a study published by Newcomer and Apt [14], suggests that the power plants should be located close to the electric load as opposed to the transport link. In reality, the location of CCS power plants will be a compromise between access to CO_2 transport infrastructure and a connection to the electricity transmission system. Another view is that, CCS infrastructure will take some time to be deployed at a large scale, so it may make more sense to increase the transport capacity in steps, instead of trying to predict the future, and increase the costs of possibly under-used CO_2 pipelines [15].

Sizing the CO_2 pipeline will require reasonably precise quantification of the amount of CO_2 that will be transported and also the thermodynamic state at which the pipeline should operate [5]. It is well recognised that the CCS plants will require to operate in a transient and load following behaviour and as a consequence of this dynamic operation, the CO_2 flowrate will follow a transient behaviour with periods of zero flow [16], [17]. Therefore, the CO_2 transport infrastructure needs to be designed in order to incorporate this variability in flow.

Given the relative proximity of the expected operating conditions for CO_2 pipeline transportation to the two-phase region, particular attention has to be paid to avoid situations where phase transition may occur. This is due to the greatly increased pressure drop as well as risks to the structure of the pipeline associated with such flows. It has been shown, for example, that the compressibility of the CO_2 close to its critical point can result in additional pressure losses which are not predicted using standard design equations [18] and that alteration of load [19] can induce phase transition during the resulting transient

flow. As such, any pipeline design must account for these scenarios through appropriately detailed modelling.

In this study we present a new methodology for the design of CO_2 transport infrastructure, explicitly accounting for the kind of transient flow that might be expected for a UK-type system in the period from 2030-2050.

The remainder of this paper is laid out as follows: we first present the CO_2 profiles for transport for 2030s, 2040s and 2050s, we then describe the process followed for the pipeline design and the optimisation problem and finally we present the results and discussion.

2. CO_2 transient behaviour of the transport network

The integration of intermittent renewable energy to the energy system will require dynamic operation of the CCS plants and therefore result in a variability of the CO_2 flowrate from the capture plant to the transport system [17]. A potential pattern for this variability is presented in Figure 1 for the 2030s, 2040s and 2050s for the UK's energy system. The manner in which these profiles were obtained is presented in detail in a separate contribution and interested readers are directed here for the specifics [17]. In brief, this study considered the deployment of CCS in the UK energy system in the period to 2050, and provided a detailed description of potential dispatch patterns of CCS plants, and the characteristic flows of CO_2 that one plant would produce and also what would be produced from a hub of three CCS power plants. This information is used to provide the starting point for our current study [17]. The first thing that we observe is that the CO_2 injection is not stable for any of the future decades. The period from 2030 to 2050 is characterised by the extensive deployment of intermittent renewable energy (iRE), complemented with thermal power plant capacity. As is usual, the iRE generation displaces the thermal power generation, leading to a decade-on-decade reduction in CO_2 production for capture and subsequent transport and storage. It can be observed from Figure 1 that the average CO_2 flow decays from an average of 3.019 kmol/s in 2030 to 2.44

kmol/s in 2050, with an increase in frequency and duration of low- or no-flow scenarios as a result. This implies that the transport system should be optimally sized and ready to absorb these fluctuations. More importantly, this shows that oversizing the CO_2 pipelines based on predictions for increased CO_2 flowrates directed to the transport network may not be practically relevant.

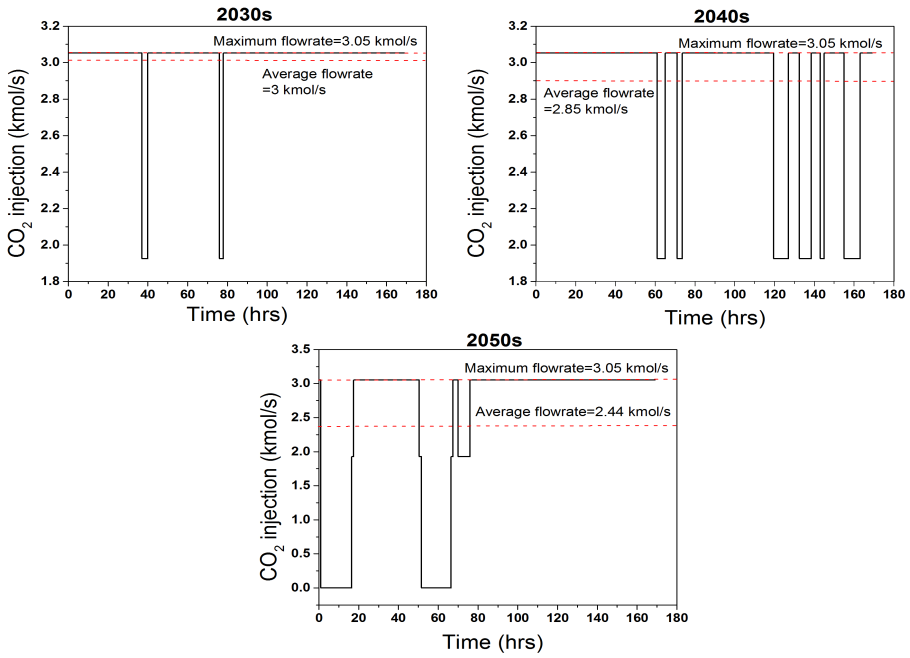

Figure 1: These graphs illustrate the transient CO_2 profiles for one CCS unit operating during 2030s, 2040s and 2050s in the UK. It is evident that the CO_2 flowrate is not stable, and actually declines with time. As we are moving towards the 2050s, the average flowrate decreases from 3.019 to 2.44 kmol/s and we observe more periods with zero flows. This declining average flow and increasing variability in flow patterns are a direct result of increasing deployment of intermittent renewable energy generation.

In Figure 2, we present the profiles for three units operating in the three different decades. Here, the assumption is that the three units are combining their flows in on hub and directing their CO_2 to a main transport line. This is judged to be what might be a typical flow pattern for a main transport line.

The main observation is that the average flowrate is decreasing for the 2050s and even the combination of the CO_2 profiles from three different units will provide the same variability to the CO_2 injection into the transport network.

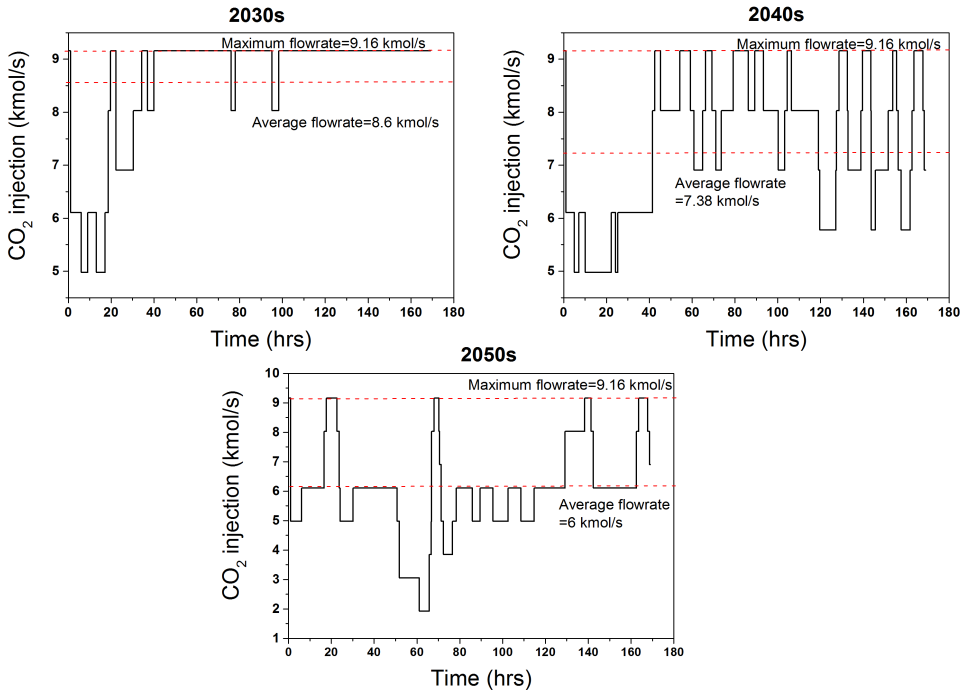

Figure 2: This graph illustrates the transient CO_2 profiles for three units operating in the 2030s, 2040s and 2050s in the UK. The most evident thing is that the CO_2 flowrate is not stable for any of the future decades. As we are moving towards the 2050s, the average flowrate is decreased to 6.019 kmol/s and we observe more periods with zero flows. This is explained by the integration of the renewable energy becoming more apparent in 2050s.

This implies that the idea of oversizing the pipelines for CO_2 transport may not be necessary, as even with increased CCS capacity deployed in the future, the co-deployment of iRE will act to reduce the average CO_2 flowrate directed to the transport network. Putting this another way, a pipeline which is sized

for the installed capacity in 2030 with an average flow of 8.6 kmol/s is already oversized relative to what would be required in the 2050s where the average flow is 6.019 kmol/s-or approximately 30% lower than in the 2030s.

3. Description of the pipeline design process

In this section we present the approach we followed to design the CO_2 pipeline. In order to do so, a cost optimisation model has been combined with one-dimension steady flow model (ODSF) in order to ensure that the cost optimal solution of the pipeline design is safe and operable, as illustrated in Figure 3. The optimisation model calculates the pipeline diameter based on a set of available diameters and CO_2 flowrate and sends this value to the pipeline ODSF flow model. The ODSF model, taking into account the detailed characteristics of the pipeline and transport fluid, then recalculates the safe and operable diameter (final diameter).

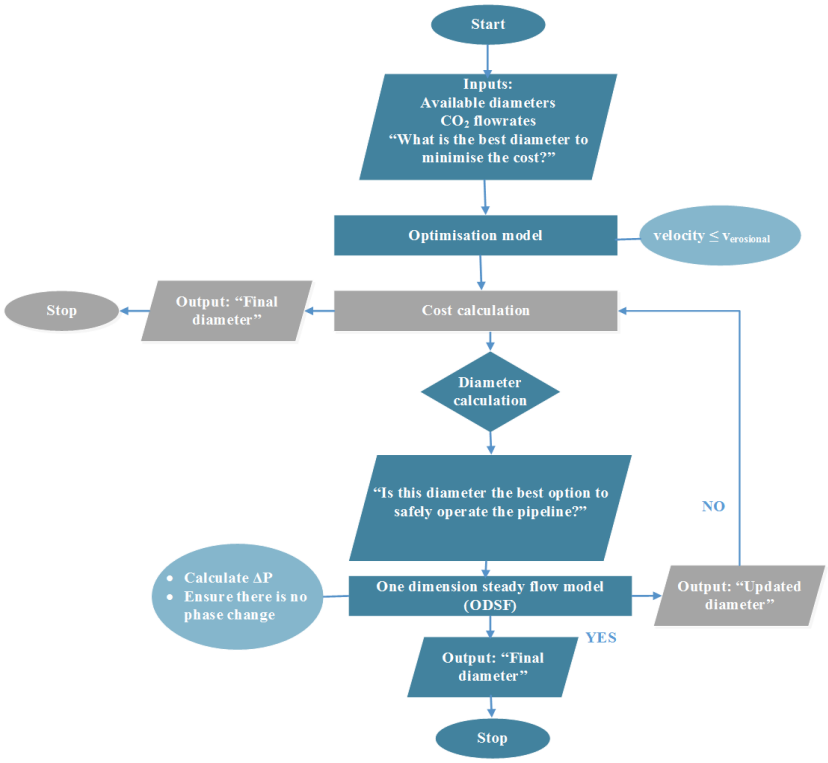

Figure 3: This figure illustrates the flow diagram which describes the interaction between the two models. The optimisation model calculates the pipeline diameter based on the available dimaters and CO_2 flowrate and sends this value to the pipeline ODSF flow. The ODSF model taking into account the detailed characteristics of the pipeline and transport fluid, re-calculates the safe and operable diameter (final diameter).

3.1. CO_2 properties for pipeline transport

CO_2 can be transported through pipelines as a liquid, gas or supercritical fluid. It is generally recommended, to transport the CO_2 in a dense or supercritical phase, where the viscosity is low and the density is high, leading to the most economical and efficient method of transport. Specifically, the CO_2 transport as a subcooled liquid state is more economical and increases the energy efficiency of the process [20]. When impurities such as as N_2, H_2, CO, water, SO_2 and NO_2 are present, the thermophysical properties of the CO_2 stream, such as

the density, the specific pressure drop and the critical point change. This will change the pipeline design such as the diameter, wall thickness, minimum allowable operating pressure (MAOP) and the distance between booster stations, leading to higher transport costs [21]. In this work, the CO_2 stream after the compression train is assumed to have a pressure of 110 bar and a temperature of 25°C (dense phase) without impurities, however in the EU the recommended CO_2 stream for transport can allow a range of impurities [22].

3.2. Pipeline design

One of the first stages in the design of a pipeline is to calculate the required internal diameter for the anticipated flowrate. In the literature, there are several models to calculate the pipeline diameter. The velocity based models [7], [23], [24],[25] are used for an initial estimation of the diameter and not for a detailed design. In this equation, the only parameters used are the velocity, mass flowrate and density. The velocity changes with respect to the pressure losses and flowrate and therefore cannot be used with confidence as an initial parameter [26]. The hydraulic equations can be used for pipelines with fluid transportation [27], [28], in case no accurate Manning coefficients are available in order to use the extensive hydraulic equation [26]. The models of McCoy and Rubin [29] and Ogden[30] can be used both for gas and liquid transport.

In this work, we have used the hydraulic equation which is based on Darcy-Weisbach fluid mechanics principles as presented in Equation 1.

$$d_i = \left(\frac{8 \cdot f_D \cdot m^2}{\pi^2 \cdot \rho \cdot \frac{\Delta P}{L}}\right)^{\frac{1}{5}} \tag{1}$$

where f_D is the Darcy friction factor, m is the mass flowrate of the fluid (kg/s), ρ is the density of the fluid (kg/m^3), L is the length of the pipeline (m) and ΔP is the overall pressure drop (Pa).

The Darcy friction factor f_D is calculated by Equation 2 ,where f_F is the Fanning friction factor.

$$f_D = 4 \cdot f_F \tag{2}$$

The Fanning friction factor is calculated from the Colebrook-White equation 3.

$$\frac{1}{2 \cdot \sqrt{f_F}} = -2.0 \cdot \log(\frac{\frac{\varepsilon}{d_i}}{3.7} - \frac{5.02}{Re} \cdot \log[\frac{\frac{\varepsilon}{d_i}}{3.7} - \frac{5.02}{Re} \cdot \log(\frac{\frac{\varepsilon}{d_i}}{3.7} + \frac{13}{Re})]) \quad (3)$$

where ε is the roughness (ε=4.57·10^{-5} m) for a carbon steel pipe [29] and Re is the Reynolds number which is calculated by Equation 4.

$$Re = \frac{4 \cdot m}{\mu \cdot \pi \cdot D_i} \quad (4)$$

where μ is the absolute dynamic viscosity of the fluid which can be assumed to be $6.06 \cdot 10^{-5}$ [Pa·s] [27] .

As can be observed from Equation 4, the internal diameter is required as an input to the calculation of Re. Therefore the pipeline diameter is calculated through an iterative process with an initial guess.

Pipelines are available in so-called nominal pipe sizes (NPS), which are related to the outer diameter other than the inlet diameter [31]. In order to relate the outer diameter to the inlet, the wall thickness can be determined using Equation 5.

$$t = \frac{P_{MOP} \cdot D_o}{2 \cdot SMYS \cdot E \cdot D.F.} \quad (5)$$

where E is the longitudinal joint factor which varies with the type of joint used in manufacturing the pipe (assumed to be equal to 1 for seamless pipe), D_o is the outer diameter (m) which is calculated by Equation 6, SMYS is the specified minimum yield stress of the pipe material, PMOP is the maximum operating pressure equal to 12.5 MPa [32] and D.F. is the design factor based on the governing code and operator specifications for the CO_2 pipeline. The SMYS depends on the pipeline material and increases as the cost of the steel pipe increases. We have chosen a value of 414 MPa which is for an X60 steel pipe [33]. The design factor, D.F, for steel pipe is a construction derating factor dependent upon the location class unit, which is an area that extends 220 yards on either side of the centerline of any continuous 1-mile length of pipeline. It

was assumed that the pipeline would be located in a Class 1 location (a Class 1 location is any 1-mile section of pipeline that has 10 or fewer buildings intended for human occupancy) and a design factor of 0.72 was used [21]. Lastly, the outer diameter, D_o, is given by Equation 6 as follows:

$$D_o = D_i + 2 \cdot t \tag{6}$$

3.3. Cost calculation process

In the literature there are several models which describe the costs for CO_2 pipelines, divided into five categories: linear models [27], [23], [28], models based on the weight of the pipeline [26], [34], quadratic equations [35], [36], the CMU model [29] and models based on flowrates [30], [7], [5]. All of these models are based on natural gas pipelines cost calculations and assume that the only pure CO_2 will be transported, *i.e.*, the models do not account for the impact of impurities in the CO_2 stream. With the presence of impurities, the material used for the pipeline has to be more expensive to increase the corrosion allowance. It is therefore preferable to transport CO_2 in as pure a form as possible using the carbon maganese steel pipelines, since other materials would be significantly more expensive. The pipeline cost models include various assumptions and are developed for different regions. For our study, we have used the quadratic model developed by the IEA GHG 2005/2, since this model has different equations for calculating onshore and offshore pipeline costs, is world oriented by including regional factors and also includes terrain factors [25].

The onshore and offshore pipeline capital costs are calculated via Equations 7 and 8. The operational and maintenance cost are assumed to be 3% of the total capital costs [25].

$$\begin{aligned} C_{onshore}^{CAPEX} = F_L \cdot F_T \cdot 10^6 \cdot [(0.057 \cdot L_{onshore} + 1.8663) \\ +(0.00129 \cdot L_{onshore}) \cdot D_o + (0.000486 \cdot L_{onshore} - 0.000007) \cdot D_o^2] \end{aligned} \tag{7}$$

$$C_{offshore}^{CAPEX} = F_L \cdot F_T \cdot 10^6 \cdot [(0.4048 \cdot L_{offshore} + 4.6946)$$
$$-(0.00153 \cdot L_{offshore} + 0.0113) \cdot D_o + (0.000511 \cdot L_{offshore} + 0.00024) \cdot D_o^2] \quad (8)$$

3.4. Formulation of the optimisation problem

When considering the design of a CO_2 pipeline, the baseline method of assessment would choose the maximum or average flowrate from the CO_2 profiles as presented in Section 2 and follow the cost calculation process as described in Section 3.3. However, this approach was developed where a steady fluid flow was anticipated. In the scenarios considered here, characterised by a declining CO_2 flow despite a increase in CCS generation capacity, this conventional approach would result in oversized infrastructure, leading to an increased cost of CCS electricity. In this study, we consider the design of pipeline with onshore and offshore segments which transports the CO_2 captured from one (and in later cases three) 500 MW unit(s) located in Selby through the Yorkshire and Humber CCS Cross Country pipeline for storage in the North Sea [37]. The onshore and offshore pipeline segments are 75km and 90km long, respectively. This case study is illustrated in Figure 4 for clarity.

Figure 4: This figure illustrates the pipeline route from the power station to the geological storage site at the North Sea. The onshore pipeline is 75km long and the offshore pipeline is 90km long. [37]

The objective function of the model is to minimise the total capital and operational costs of the pipeline by selecting the optimal outlet diameter available from the database of the nominal pipe sizes [31]. The objective function is formulated as follows:

$$minC_{TOTAL} = \sum_{d} Y_d \cdot (C^{CAPEX}_{onshore} + C^{CAPEX}_{offshore} + C^{O\&M}_{onshore} + C^{O\&M}_{offshore}) \quad (9)$$

When designing the pipeline by selecting the optimal diameter and thickness, we need to ensure that the erosion is not a threat to the pipe. This is the constraint to the optimisation problem and is expressed by Equation 10.

$$\sum_{d} v_{h,d} \cdot Y_d \leq v_e \qquad \forall h \quad (10)$$

where v_h is the velocity of the CO_2 for different hours during the optimisation

period, Y_d is a binary variable and the subscript d are the different available diameters.

The erosional velocity is calculated by Equation 11 [38]:

$$v_e = \frac{\sqrt{8 \cdot \tau_w}}{\sqrt{f_D} \cdot \sqrt{\rho}} \tag{11}$$

where τ_w is the shear on the pipe (40 N/m^2), ρ is the density of the fluid in kg/m^3 and f_D is the average value of the friction factor (0.013), which is calculated by Equation2 using the different available diameters based on our case studies. The value of the friction factor is a very important parameter in the optimisation problem since it contributes to the calculation of the erosional velocity which is the constraint on the optimisation problem. Higher values of the f_D will result in lower values of v_e in turn affecting the selection of the optimal diameter. In our case, we have defined the region of diameters in which the solution would be based on the flowrate variations and we have calculated the average value of f_D.

The velocity of the CO_2 through the pipeline is calculated by the continuity equation as described in Equation 12.

$$v_h = \frac{4 \cdot m_h}{\pi \cdot \rho \cdot D_o^2} \qquad \forall h \tag{12}$$

where m_h is the mass flowrate of the CO_2 for different hours h during the optimisation period.

Finally, one only diameter can be selected:

$$\sum_d Y_d = 1 \tag{13}$$

The problem described above results in an MINLP model which is modelled and solved in GAMS using the CONOPT solver [39].

3.5. Rigorous steady-state calculations

The approach as described above allows the selection of the optimal pipeline diameter and thickness, however the assumption of incompressible flow within

the hydraulic model may result in errors close to the critical point [18]. The analysis of Martynov et al. [18] shows that for the feed pressure assumed in this study this error may be significant, in order that a viable diameter and thickness are selected the optimised configuration is simulated using a rigorous steady-state flow model [10, 18]. To describe the compressible flow and heat transfer of a single-phase fluid in long pipelines the one-dimensional steady-state flow (ODSF) model describes employs the following equations for mass, momentum and energy conservation respectively:

$$\frac{d\rho v}{dx} = 0 \tag{14}$$

$$\frac{d\rho v^2 + P}{dx} = -2f_F \frac{\rho v^2}{D_i} \tag{15}$$

$$\frac{d\rho v \left(h + \frac{1}{2}u^2\right)}{dx} = \frac{4q_w}{D_i} - 2f_F \frac{\rho v^3}{D_i}. \tag{16}$$

where x is the local coordinate along the pipeline, f_F is the Fanning friction factor and q_w is the heat flux at the pipewall. q_w is defined via:

$$q_w = \alpha \left(T_f - T_a\right) \tag{17}$$

where T_f and T_a are the temperatures of the fluid and the ambient soil, the definition of an overall heat transfer coefficient, α [18].

3.6. Operability of the pipelines

Once the thickness of the pipeline has been determined using the steady state analysis detailed in the previous section, the transient fluid flows arising from the dynamic source profiles are analysed to ensure that in these cases no unwanted behaviour, such as phase transition, is encountered. Such analysis is performed by applying the time-dependent variant of the system of equations 14-16 [40, 41]:

$$\frac{\partial \rho}{\partial t} + \frac{\partial \rho v}{\partial x} = 0 \tag{18}$$

$$\frac{\partial \rho v}{\partial t} + \frac{\partial \rho v^2 + P}{\partial x} = -2 f_F \frac{\rho v^2}{D_i} \tag{19}$$

$$\frac{\partial E}{\partial t} + \frac{\partial \rho v \left(h + \frac{1}{2}u^2\right)}{\partial x} = \frac{4 q_w}{D_i} - 2 f_F \frac{\rho v^3}{D_i}. \tag{20}$$

To solve equations 18-20 numerically, a finite volume method is used [42], where following Brown et al. [10], the conservative left-hand-side of equations 18-20 are solved using the AUSM-+ flux vector splitting scheme [43].

4. Results and discussion

4.1. Results of the optimisation problem

The optimisation problem described in the previous section has been solved taking into account the varying CO_2 flowrates for one and three units characteristic of the 2030s, 2040s and 2050s as described in section 2. The results for the one and three units are presented in Table 1.

Table 1: In this table we present the results of the optimisation problem compared to designing the pipeline for the maximum flowrate as it evaluated for the 2030s. We observe 39% savings for the one unit and 52.9% savings for the three units.

Unit 1	C_{TOTAL} (£)	D_o (m)	Savings (%)
Optimisation	59,691,140	0.2191	39
Maximum flow	97,954,965	0.559	-
3 Units	C_{TOTAL} (£)	D_o (m)	Savings (%)
Optimisation	69,709,420	0.3556	52.9
Maximum flow	148,000,000	0.813	-

In figure , the outside diameters D_o and wall thicknesses t are given based on API available sizes [31]. The red stars are the results of the optimisation while the blue crosses are the results calculated based on the maximum flowrate.

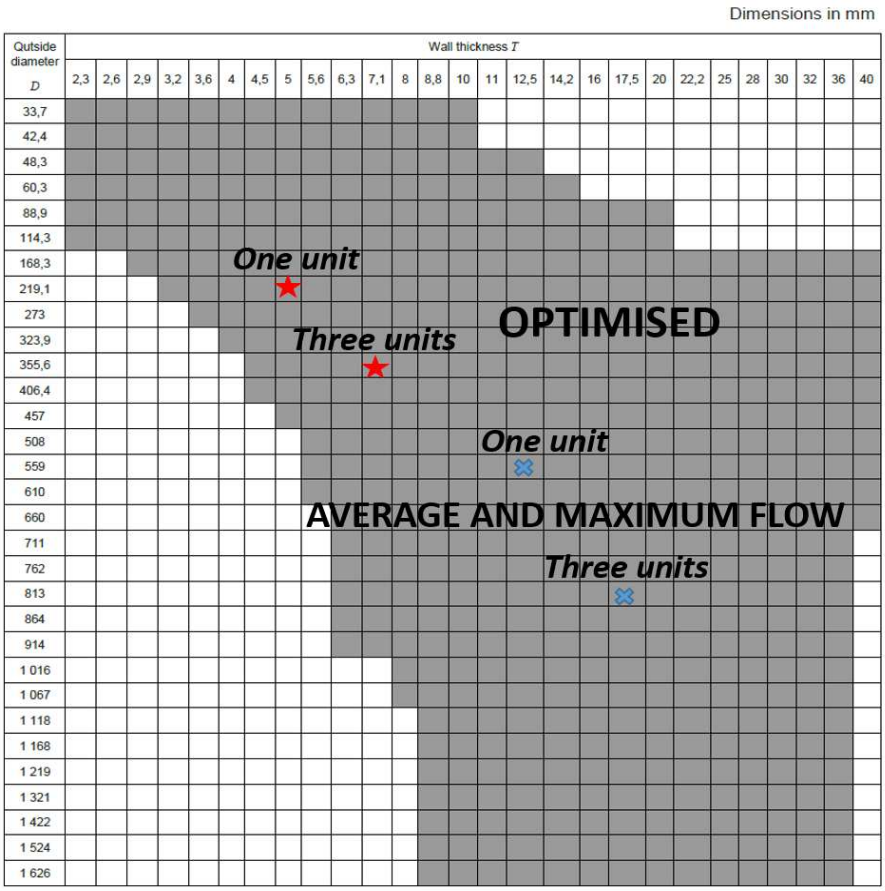

Figure 5: This figure illustrates the available combinations of external diameters and wall thicknesses for steel pipelines for CO_2 transport. The red star presents the optimisation results while the blue crosses are the results based on maximum (or average) flowrate. Significant decrease of the pipeline diameter which leads to decrease of costs.

Following the same procedure for sizing for the 2040s and 2050s, we arrive at the same results since the maximum flowrate remains the same while the average flowrate decrease throughout the years does not lead to a different

diameter selection from the available sizes.

4.2. Steady state problem

Following the calculation of the optimal pipeline design as described in the previous section, the rigorous ODSF was applied to more accurately calculate the pressure drop, analysis is presented for the one unit scenario. It was found that for the external diameters selected at the maximum flowrate the pressure drop was such that the CO_2 would change phase; to correct the design for this, the external diameter was increased while keeping the wall thickness constant until an acceptable pressure drop was obtained. A pipeline with a diameter of 0.4064m with the same thickness gives a 10bar cushion from the critical point. A similar analysis for the three unit case showed that a diameter of 0.610m provided the same level of conservativeness. Furthermore, given the impact of heat transfer close to conditions of interest here shown in the analysis of Martynov et al. [18], the temperature of the surrounding soil was varied to temperatures representative of winter and summer (the maximum and minimum) as well as a yearly average, which were obtained by an *a priori* calculation of the steady heat conduction in the soil using real ambient temperature data [44]. These are based on sandy soil and data taken for the whole of the UK. For the sake of brevity, only the results for the one unit case are presented below.

Figures 6 (a) and (b) show the predicted variation of the pressure along the length of the pipeline for the various soil temperatures tested for the minimum and maximum flowrates observed for the 2030s scenario. As can be seen, the pressure drop is linear in both cases with that calculated for the maximum flowrate being approximately three times that of the minimum, while the external temperature is seen to have a minimal impact on the pressure drop in either case.

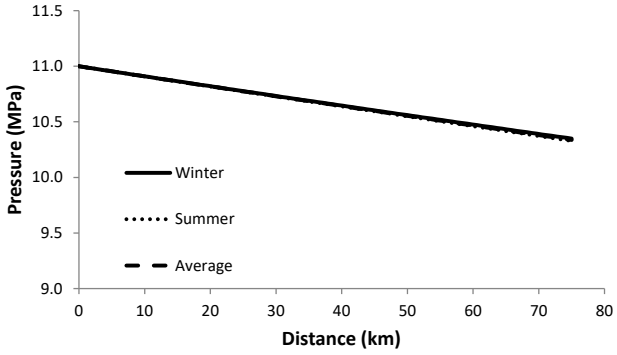

(a)

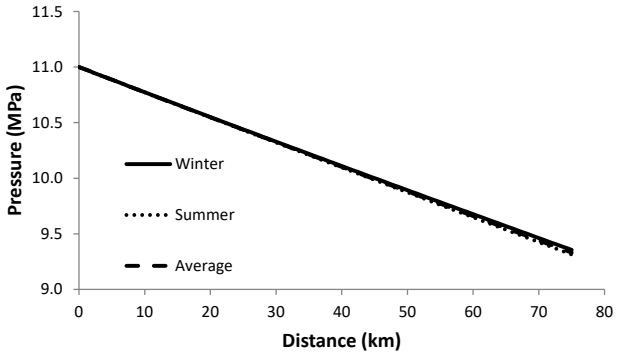

(b)

Figure 6: This figure presents the variation of pressure along the pipeline length for the (a) minimum and (b) maximum flowrates, assuming soil temperatures indicative of winter, summer and a yearly average (275.25, 288.85 and 283.45 K respectively)

Similarly, Figures 7 (a) and (b) show the predictions of the fluid temperature, also along the length of the pipe for the various external soil conditions, for the minimum and maximum flowrates respectively. Unlike the pressure, the temperature is markedly affected by the external temperature with the delivery temperature in each case approaching that assumed for the surrounding soil. In neither case is this sufficient to induce phase change, however.

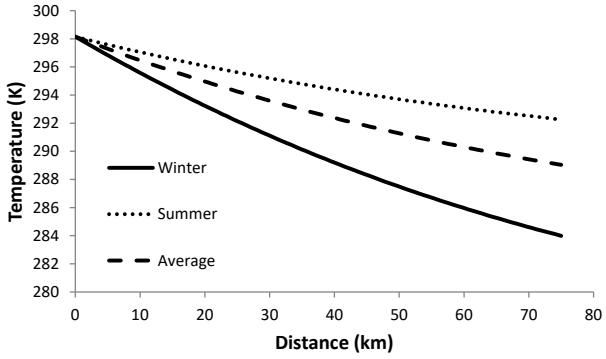

(a)

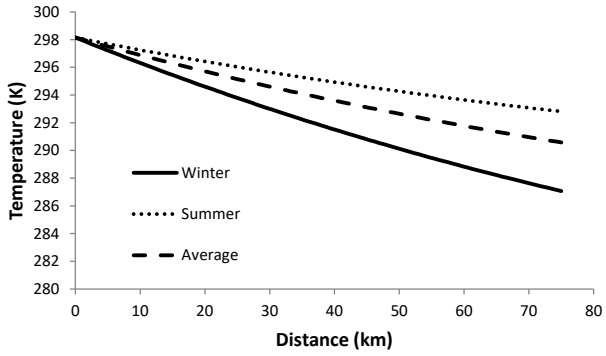

(b)

Figure 7: This figure presents the variation of pressure along the pipeline length for the (a) minimum and (b) maximum flowrates, assuming soil temperatures indicative of winter, summer and a yearly average (275.25, 288.85 and 283.45 K respectively)

4.3. Transient flow model

While the analysis presented above focuses on the design of the pipeline under steady loads, it is essential that the final system design is appropriate for the transient conditions during the predicted load changes over all of the periods under consideration. As such, for the production profile for the one unit scenario in the 2030s as presented in Figure 1 the first 48 hours of flow is simulated using the transient flow model presented in the Section 3.6. It should be observed that this time period contains the same load change seen in the later periods but does not contain a cessation of the flow; as this latter operation lies outside of normal use of the pipe it is not studied here in detail.

In addition to the pipeline characteristics presented, for the purposes of the simulations, 200 computational cells were used and an ambient temperature undergoing a diurnal change is applied. As with the steady state simulations, ambient temperatures representing summer, winter and a yearly average (293.15, 277.15 and 285.15K respectively) are used .

Figures 8 and 9 present the variation of the temperature and pressure at the delivery end of the pipeline respectively. As may be observed from Figure 8, a slight drop in the temperature occurs where the ramp-down can be observed at ca. 37 h; in each of the cases studied the diurnal temperature change is far greater than observed during the load change. Likewise in Figure 9 the pressure is observed to drop during the load change, the degree of this is in this case much larger than that induced by the diurnal variation; however, this change is small relative to the drop along the length of the pipeline. Importantly, given the design selected, the transients do not result in unwanted behaviour such as

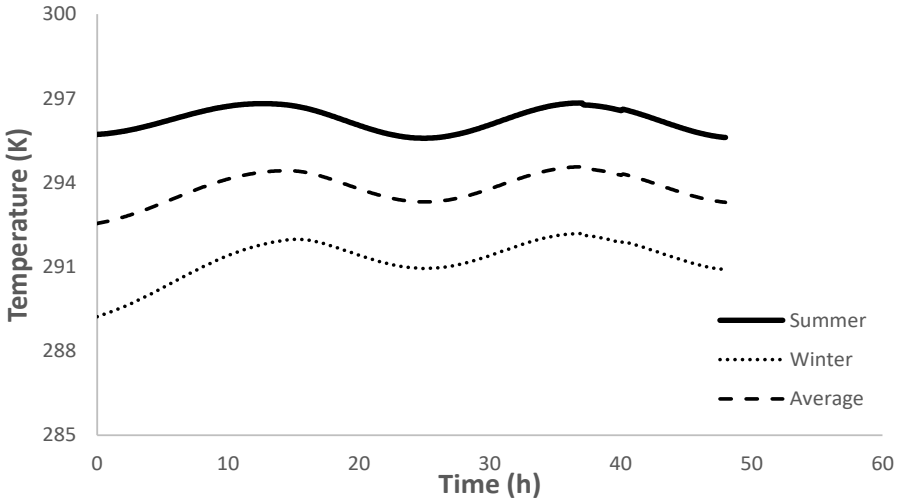

Figure 8: This figure presents the variation of temperature at the delivery end of the pipeline. A slight drop in the temperature occurs where the ramp-down can be observed at ca. 37 h; in each of the cases studied the diurnal temperature change is far greater than observed during the load change.

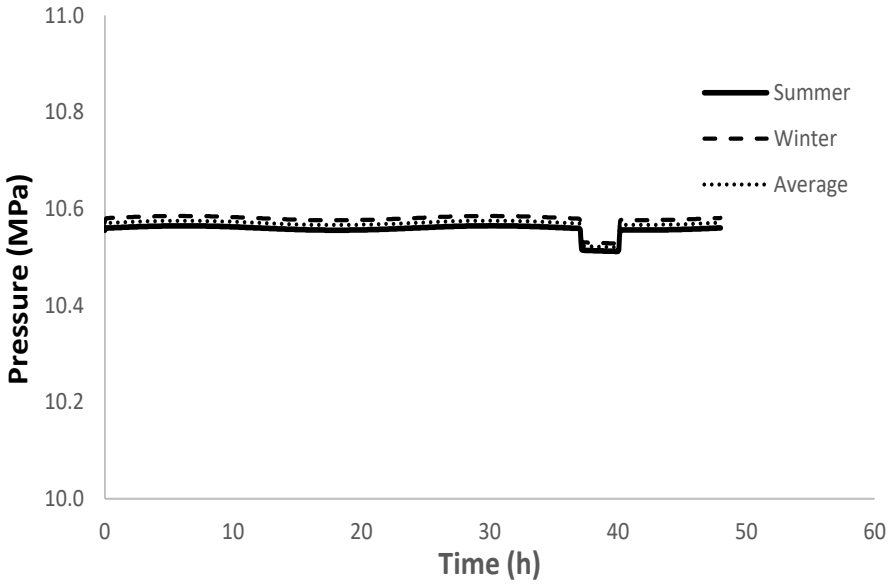

Figure 9: This figure presents the variation of pressure at the delivery end of the pipeline. The pressure is observed to drop during the load change, the degree of this is in this case much larger than that induced by the diurnal variation; however, this change is small relative to the drop along the length of the pipeline.

4.4. A trade-off between safety and cost

The updated results based on the two combined models for one unit and three units in the 2030s are presented in Figure 10. The updated results which take into consideration the safety and operability of the pipeline, according to the methodology laid out in Section 3.6 suggest a pipeline of 0.406m with 0.005m thickness compared to the result of the optimisation problem of 0.219m with the same thickness for the one unit. This leads to reduction of the cost savings from 39% to 22% compared to the base case. For the three units, the results of the combined ODSF and optimisation model lead to a 28.3 % reduction compared to a 52.9 % reduction as a result of the optimisation problem. This combination of the detailed transport model and high level optimisation model, can therefore ensure the cost optimal and safe design and operation of a CO_2 pipeline.

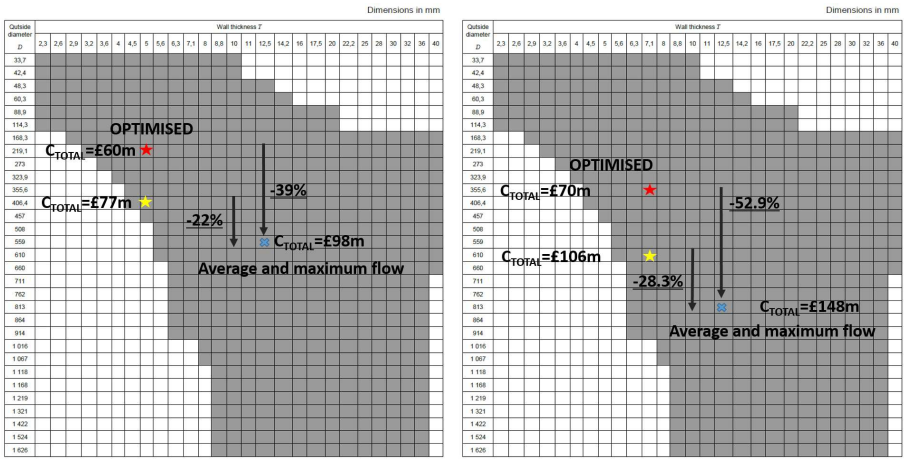

(a) One Unit in 2030s.

(b) Three Units in 2030s.

Figure 10: This figure illustrates the updated results on right-sizing the CO_2 pipeline combining the optimisation and ODSF model for one and three units in 2030s. The red star is the result of the optimisation problem, the blue cross is the diameter calculated based on maximum and average flowrate and the yellow star is the result of the ODSF model. In order to have a safe and operable pipeline the cost saving is reduced to 22 % and 28.3 % for one and three units respectively, but still remains significant.

5. Conclusions

We have presented a new approach on designing the CO_2 transport pipeline. An optimisation problem for the optimal design of the CO_2 transport pipeline has been solved combined with a detailed transport model (ODSF-One dimension steady flow model) to ensure the safe operation of the selected pipeline during transient flows. We have solved this problem for the 2030s for the UK. The algorithm's solution showed that even cost reduction up to 53% can be achieved with optimal pipeline sizing. Checking the solution with the detailed ODSF model led to increased pressure drop occured by the selected diameter inducing two phase flow and therefore a larger pipeline has been selected. The same results have been obtained for the 2040s and 2050s due to the same maximum and decreased average flowrates for the three decades showing that the

pipeline design selected for the 2030s can be used to accommodate the CO_2 flowrates for the future. The final cost reduction is 22 % and 28.3 % for one and three units respectively. In this way, we have challenged the conventional assumption that initial oversizing CO_2 transport infrastructure is key to achieving a least-cost system over the longer term. Whilst it true to say that infrastructure must be deployed with an eye to the future, accounting for the CCS plants that will subsequently be deployed, it is equally true that the likely operation of these plants within the kind of energy system that is likely to exist should also be taken into account. In this study, we have demonstrated that where CCS plants are deployed in an energy system characterised by extensive deployment of intermittent renewable energy (iRE), the resulting displacement of CCS power plant generation by iRE generation leads to a decade-on-decade declining flow of CO_2 through the transport infrastructure, despite a concurrent increase in the quantity of CCS capacity deployed. This means that the right-sizing of CO_2 transport infrastructure via the approach set out in this study can lead to non-negligible reductions in infrastructure cost without compromising the ability to accommodate future capacity or safety. We therefore suggest that when CCS infrastructure is being designed for deployment at a national or supra-national scale, with the associated deployment of CO_2 transport networks, as distinct to the point-to-point lines discussed in this work, a similar approach of combining energy system simulations with engineering modelling and optimisation should become the norm. We contend that this novel approach has the potential to lead to appreciable cost reductions in the deployment of a truly fit for purpose infrastructure.

6. Acknowledgements

The authors gratefully acknowledge the financial support of the grant EP/M001369/1 MESMERISE-CCS.

7. References

[1] Technology Roadmap, Carbon Capture and Storage, 2013 edition, https://www.iea.org/publications/freepublications/publication/technology-roadmap-carbon-capture-and-storage-2013.html. *IEA-GHG*.

[2] M. E. Boot-Handford, J. C. Abanades, E. J. Anthony, M. J. Blunt, S. Brandani, N. Mac Dowell, J. R. Fernandez, M. C Ferrari, R. Gross, J. P. Hallett, R. S. Haszeldine, P. Heptonstall, A. Lyngfelt, Z. Makuch, E. Mangano, R. T. J. Porter, M. Pourkashanian, G. T. Rochelle, N. Shah, Joseph G. Yao, and P. S. Fennell. Carbon capture and storage update. *Energy and Environmental Science*, 7:130 – 189, 2014.

[3] H. Mahgerefteh, S. Brown, and G. Denton. Modelling the impact of stream impurities on ductile fractures in CO_2 pipelines. *Chemical Engineering Science*, 74:200 – 210, 2012.

[4] D. G. Jones and A. Cosham. Fracture-propagation control in dense-phase CO_2 pipelines. *Journal of Pipeline Engineering*, 7:281 – 292, 2008.

[5] M. M. J. Knoope, A. Ramrez, and A. P. C. Faaij. A state-of-the-art review of techno-economic models predicting the costs of CO_2 pipeline transport. *International Journal of Greenhouse Gas Control*, 16:241 – 270, 2013.

[6] Building Essential Infrastructure for Carbon Capture and Storage, Report to the Global Carbon Capture and Storage Institute, March 2011. *Insight Economics*.

[7] M.K. Chandel, L.F. Pratson, and E. Williams. Potential economies of scale in CO_2 transport through use of a trunk pipeline. *Energy Conversion and Management*, 51:2825 – 2834, 2010.

[8] A. Alhajaj, N. Mac Dowell, and N. Shah. Multiscale design and analysis of CO_2 capture, transport and storage networks. *Energy Procedia*, 37:2552 – 2561, 2013.

[9] N. Mac Dowell, Alhajaj A., M. Konda, and N. Shah. Multiscale whole-systems design and analysis of CO_2 capture and transport networks. *Computer Aided Chemical Engineering*, 29:1205 – 1209, 2011.

[10] S. Brown, H. Mahgerefteh, S. Martynov, V. Sundara, and N. Mac Dowell. A multi-source flow model for CCS pipeline transportation networks. *International Journal of Greenhouse Gas Control*, 43:108 – 114, 2015.

[11] T. Dixon, K. Yamaji, Z. Wang, G. I. Cardenas, G. A. Fimbres Weihs, and D. E. Wiley. Optimal Pipeline Design with Increasing CO_2 Flow Rates. *Energy Procedia*, 37:3089 – 3096, 2013.

[12] J. Gale, C. Hendriks, W. Turkenberg, J. Morbee, J. Serpa, and E. Tzimas. Optimal planning of CO_2 transmission infrastructure: The JRC InfraCCS tool. *Energy Procedia*, 4:2772 – 2777, 2011.

[13] R. S. Middleton and J. M. Bielicki. A scalable infrastructure model for carbon capture and storage: SimCCS. *Energy Policy*, 37:1052 – 1060, 2009.

[14] A. Newcomer and J. Apt. Implications of generator siting for CO_2 pipeline infrastructure. *Energy Policy*, 36:1776 – 1787, 2008.

[15] NERA (2009), Developing a Regulatory Framework for CCS Transportation Infrastructure, Vol 1, Report for DECC, London, June.

[16] N. Mac Dowell and N. Shah. The multi-period optimisation of an amine-based CO_2 capture process integrated with a super-critical coal-fired power station for flexible operation. *Computers and Chemical Engineering*, 74:169 – 183, 2015.

[17] N. Mac Dowell and I. Staffell. The role of flexible CCS in the UK's future energy system. *International Journal of Greenhouse Gas Control*, 48, Part 2:327 – 344, 2016.

[18] S. Martynov, N. Mac Dowell, S. Brown, and H. Mahgerefteh. Assessment of Integral Thermo-Hydraulic Models for Pipeline Transportation of Dense-Phase and Supercritical CO_2. *Industrial & Engineering Chemistry Research*, 54:8587 – 8599, 2015.

[19] S. Liljemark, K. Arvidsson, M. T. P McCann, H. Tummescheit, and S. Velut. Dynamic simulation of a carbon dioxide transfer pipeline for analysis of normal operation and failure modes. *Energy Procedia*, 4:3040 – 3047, 2011.

[20] Z. X. Zhang, G. X. Wang, P. Massarotto, and V. Rudolph. Optimization of pipeline transport for CO_2 sequestration. *Energy Conversion and Management*, 47:702 – 715, 2006.

[21] T. Dixon, H. Herzog, S. Twinning, B. Wetenhall, H. Aghajani, H. Chalmers, S. D. Benson, M-C. Ferrari, J. Li, J. M. Race, P. Singh, and J. Davison. Impact of CO_2 impurity on CO_2 compression, liquefaction and transportation. *Energy Procedia*, 63:2764 – 2778, 2014.

[22] Wilcox Jennifer, Carbon Capture, London, Springer, 2012.

[23] Element Energy. CO_2 pipeline infrastructure: An analysis of global challenges and opportunities. Final report for IEA Greenhouse Gas Programme, 1-134, 2010.

[24] T. Kazmierczak, R. Brandsma, F. Neele, and C. Hendriks. Algorithm to create a CCS low-cost pipeline network. *Energy Procedia*, 1:1617 – 1623, 2009.

[25] Building the cost curves for CO_2 storage: European sector. Report Number 2005/2. International Energy Agency Greenhouse Gas R&D Programme. *IEA-GHG*, 2005.

[26] K. Piessens, B. Laenen, W. Nijs, P. Mathieu, J.M. Baele, et al., 2008. Policy Support System for Carbon Capture and Storage.SD/CP/04A, 1 269.

[27] G. Heddle, H. Herzog, and M. Klett. The economics of CO_2 storage. *2003, MIT LFEE 2003-003 RP, 1 - 115.*

[28] M. van den Broek, A. Ramrez, H. Groenenberg, F. Neele, P. Viebahn, W. Turkenburg, and A. Faaij. Feasibility of storing CO_2 in the Utsira formation as part of a long term dutch CCS strategy: An evaluation based on a GIS/MARKAL toolbox. *International Journal of Greenhouse Gas Control*, 4:351 – 366, 2010.

[29] S. T. McCoy and E. S. Rubin. An engineering-economic model of pipeline transport of CO_2 with application to carbon capture and storage. *International Journal of Greenhouse Gas Control*, 2:219 – 229, 2008.

[30] D. L. McCollum, J. M. Ogden, 2006. Techno-economic models for carbon dioxide compression, transport, and storage & Correlations for estimating carbon dioxide density and viscosity. UCD-ITS-RR-06-14, 1 - 87.

[31] BS EN10208-2, 2009. BS EN 10208-2, Steel pipes for pipelines for combustible fluids. Technical delivery conditions. Pipes of requirement class B British Standards Institute, London.

[32] N. Ghazi and J. M. Race. Techno-economic modelling and analysis of CO_2 pipelines. *Proceedings of the 2012 9th International Pipeline Conference IPC2012, September 24-28, 2012, Calgary, Alberta, Canada.*

[33] M. M. J. Knoope, W. Guijt, A. Ramrez, and A. P. C. Faaij. Improved cost models for optimizing CO_2 pipeline configuration for point-to-point pipelines and simple networks. *International Journal of Greenhouse Gas Control*, 22:25 – 46, 2014.

[34] L. Gao, M. Fang, H. Li, and J. Hetland. Cost analysis of CO_2 transportation: Case study in china. *Energy Procedia*, 4:5974–5981, 2011.

[35] Pipeline transmission of CO_2 and energy. Transmission study report. PH4/6, 1 - 140. *IEA-GHG*, 2002.

[36] N. Parker, 2004. Using natural gas transmission pipeline costs to estimate hydrogen pipeline costs. UCD-ITS-RR-04-35, 1-85.

[37] Yorkshire and Humber CCS Project, National Grid,www.ccshumber.co.uk.

[38] API14E, 1991. Recommended practice for design and installation of offshore production platform piping systems (5th Edition). American Petroleum Institute, Washington, DC.

[39] A. Brooke, D. Kendrick, A. Meeraus and A. Raman. GAMS-A User's Guide. GAMS Development Corporation 2008.

[40] S. Brown, J. Beck, H. Mahgerefteh, and E. S. Fraga. Global sensitivity analysis of the impact of impurities on CO_2 pipeline failure. *Reliability Engineering and System Safety*, 115:43 – 54, 2013.

[41] H. Mahgerefteh, S. Brown, and S. Martynov. A study of the effects of friction, heat transfer, and stream impurities on the decompression behavior in CO_2 pipelines. *Greenhouse Gases: Science and Technology*, 2(5):369 – 379, 2012.

[42] R. J. Leveque. *Finite Volume Methods for Hyperbolic Problems*. Cambridge University Press, Cambridge, 2002.

[43] M. Liou. A sequel to AUSM, Part II: AUSM+-up for all speeds. *J. Comput. Phys.*, 214(1):137–170, 2006.

[44] UK meteorological office, http://www.metoffice.gov.uk/ (Accessed 30 October 2016).